energies

MDPI

Article

Downsizing Sustainable Aviation Fuel Production with Additive Manufacturing—An Experimental Study on a 3D printed Reactor for Fischer-Tropsch Synthesis: Supplementary Information

David F. Metzger [1,*], Christoph Klahn [2] and Roland Dittmeyer [1]

[1] Institute for Micro Process Engineering (IMVT), Karlsruhe Institute of Technology (KIT), Herrmann-von-Helmholtz-Platz 1, 76344 Eggenstein-Leopoldshafen, Germany
[2] Institute of Mechanical Process Engineering and Mechanics (MVM), Karlsruhe Institute of Technology (KIT), Strasse am Forum 8, 76131 Karlsruhe, Germany
* Correspondence: david.metzger@kit.edu; Tel.: +49-721-608-23047

Materials

The materials employed in the experiments are described in Table S1.

Table S1: Materials.

Name	Company	Product
Male threaded connectors	Swagelok	SS-6M0-1-2RS, SS-12M0-1-8RS
Metal gasket	Swagelok	304L-2-RSNB-2, 304L-8-RSNB-2
Sinter metal	GKN	SIKA-R 100 AX, $t = 2$ mm
Graphite sealing	Frenzelit	Novaphit VS, $t = 2$ mm
Thermocouples	Conatex	Type K (NiCr-Ni) OD 0.5 mm; 1 mm
Heating cartridges	Kleinesdar	OD ¼", 100 W @ 230 VAC
Thermal conductivity paste	IBF Chemotechnik Elektronik GmbH	Ferotherm 4
Mass flow controllers (MFC)	Brooks	$\dot{V}_{N2} = 30\frac{mL_N}{min}$; $\dot{V}_{H2} = 600\frac{mL_N}{min}$; $\dot{V}_{CO} = 300\frac{mL_N}{min}$
Oil thermostat	Lauda	Proline P12C
Thermal oil	Fragol	Fragoltherm 660
Insulation material	Isover	U Protect Pipe Sect- Alu2
Preprocessing software	DMG MORI	RDesigner (version 1.23.01, Revision 2017)
Printer operating Software	DMG MORI	ROperator (version 1.0.2.376, Revision 943 (2018))
Printer	DMG MORI	Realizer SLM 125
Purge gas	Air Liquide	Argon 5.0
Metal powder	Carpenter Additive	CT PowderRange 316LF
NC mill	Deckel	FP5
Laboratory scale	Kern und Sohn	ABS-N ABJ-NM

AM Scan Strategy

Table S2 contains details on the additive manufacturing strategy employed in this work.

Table S2: Scan strategy: order and details of features.

Detail	Value	Unit
0. General		

Heating	True	
h_{layer}	0.05	mm
Heat function	True	
	1. Hatch	
Exposure time *ET*	10	µs
Point distance *PD*	10	µm
Scan velocity *SV*	1	m s^{-1}
Power *P*	110	W
Lens position *LP*	0.6	mm
To 1. Advanced hatch definition		
Initial offset	0.12	mm
Hatch distance	0.08	mm
Rotation	93	°
Scan direction	Alternating	
Multiply method	Random	
Shifted	True	
Patch size	8 x 5	mm
2.+3. Fill line		
ET	50	µs
PD	10	µm
SV	0.2	m s^{-1}
P	110	W
LP	0.2	mm
Base offset	0.08	mm
4.+5. Inner contours, 6.+7. outer contours		
ET	50	µs
PD	10	µm
SV	0.2	m s^{-1}
P	110	W
LP	0.2	mm

AM Porous Region

Preliminary tests revealed for the hydrodynamic behavior of the frit the following values according to ISO 4022 [1]: $\Psi_V = 0.5 \cdot 10^{-12}$ m^2 and $\Psi_I = 0.1 \cdot 10^{-6}$ m. This relates to a pressure drop at T = 234 °C, p = 20 bar and F = 30 L_N h^{-1} of Δp = 1000 Pa. The pressure drop of a packed bed with d_P = 100 µm and ε = 0.5 is negligible.

Test Rig

In Figure S*1* the process flow diagram of the test rig is shown.

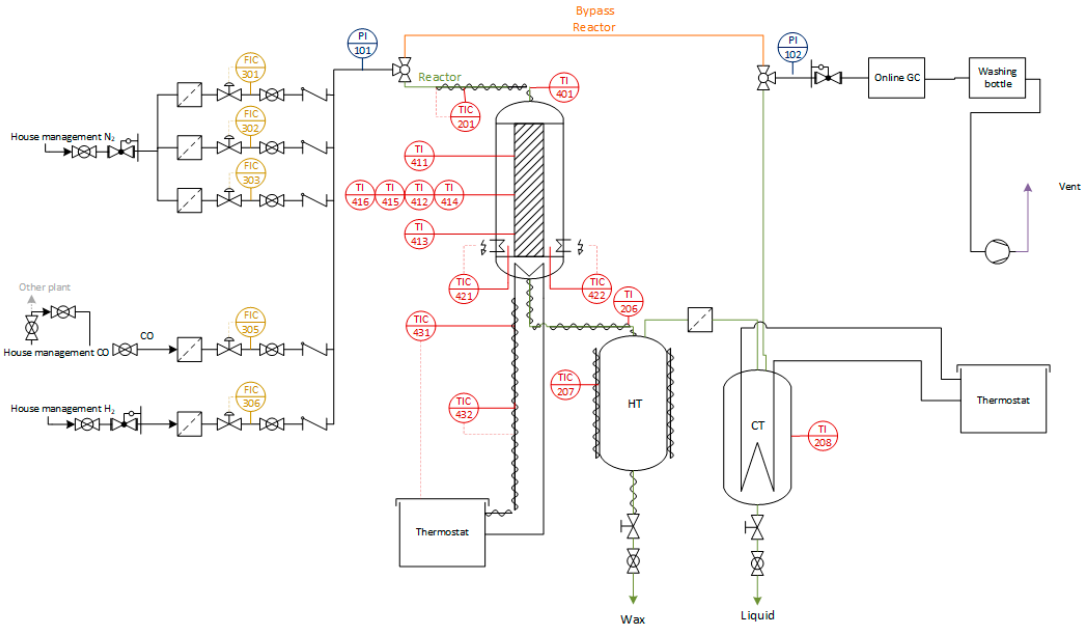

Figure S1: Process flow diagram of test rig.

In Figure S2 the test rig and reactor are shown. The connection of the oil thermostat to the reactor is clearly visible.

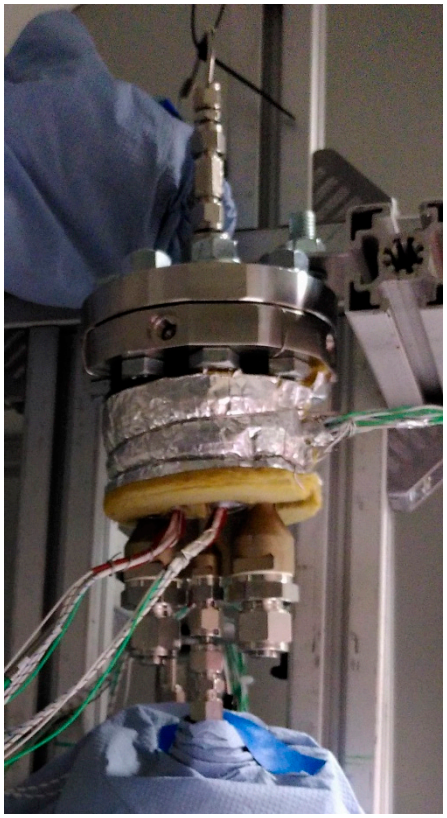

Figure S2: Reactor in test rig. Left: Reactor partially insulated. Right: Reactor (very top) insulated, oil lines and thermostat (bottom) connected.

GC Results and Product Distribution

Calculating molar flows from online GC: $\dot{N}_{i,out} = y_{i,out} \cdot \frac{\dot{N}_{N2}}{y_{N2,out}}$. Mass fraction of component with i C atoms ω_i [2,3] correlates with signal area in oil and wax GC [2,4]:

$$\omega_\mathrm{i} = \frac{A_\mathrm{i}}{\sum_{i=a}^{b} A_\mathrm{i}}$$

$$\omega_\mathrm{i} = i \cdot (1-\alpha)^2 \cdot \alpha^{\mathrm{i}-1}$$

$$\alpha = \frac{i-1}{i} \cdot \frac{\omega_\mathrm{i}}{\omega_{\mathrm{i}-1}}$$

Molar fraction of component with i C atoms x_i [5,6]: $x_\mathrm{i} = (1-\alpha) \cdot \alpha^{\mathrm{i}-1}$. Molar mass of alkane with i C atoms: $\widetilde{M}_i = i \cdot \widetilde{M}_C + (2 \cdot i + 2) \cdot \widetilde{M}_H$; $\frac{\widetilde{M}_i}{i \cdot \widetilde{M}_C} = \cdots for\ i \to \infty = 1.17$

Conversion over TOS

The CO conversion over time on stream is depicted in Figure S3.

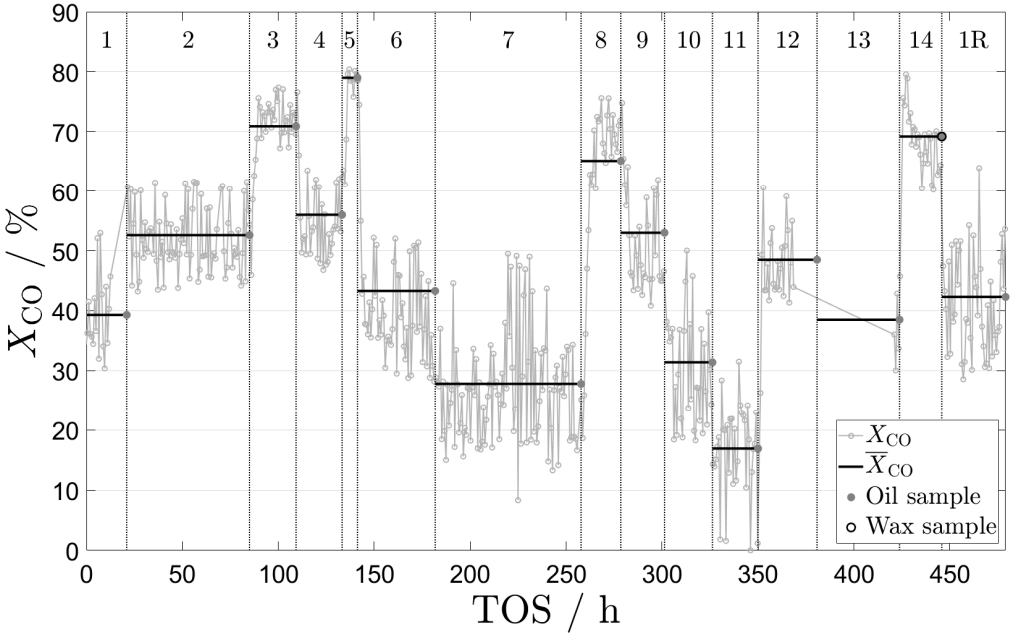

Figure S3: CO conversion over time on stream. Between setpoints 12 and 13 was an extended GC shutdown.

Fit of Conversion to Temperature and Space Velocity

The experimental data was fitted with the following fit: $\hat{X}_{\mathrm{CO,fit}} = a + b \cdot \widehat{SV}_\mathrm{mod} + c \cdot \hat{T}$ with $\hat{X}_{\mathrm{CO,fit}} = \frac{X_\mathrm{CO}^\mathrm{max} - X_\mathrm{CO}}{X_\mathrm{CO}^\mathrm{max} - X_\mathrm{CO}^\mathrm{min}}$ and $\widehat{SV}_\mathrm{mod} = \frac{SV_\mathrm{mod}^\mathrm{max} - SV_\mathrm{mod}}{SV_\mathrm{mod}^\mathrm{max} - SV_\mathrm{mod}^\mathrm{min}}$ and $\hat{T} = \frac{T^\mathrm{max} - T}{T^\mathrm{max} - T^\mathrm{min}}$ and $X_\mathrm{CO}^\mathrm{max} = 85$ and $X_\mathrm{CO}^\mathrm{min} = 10$ and $SV_\mathrm{mod}^\mathrm{max} = 10$ $SV_\mathrm{mod}^\mathrm{min} = 10$ and $T^\mathrm{max} = 240$ and $T^\mathrm{max} = 185$ and $a = 0.1868$ and $b = 1.3446$ and $c = -0.7421$. The quality of the fit is depicted in Figure S4.

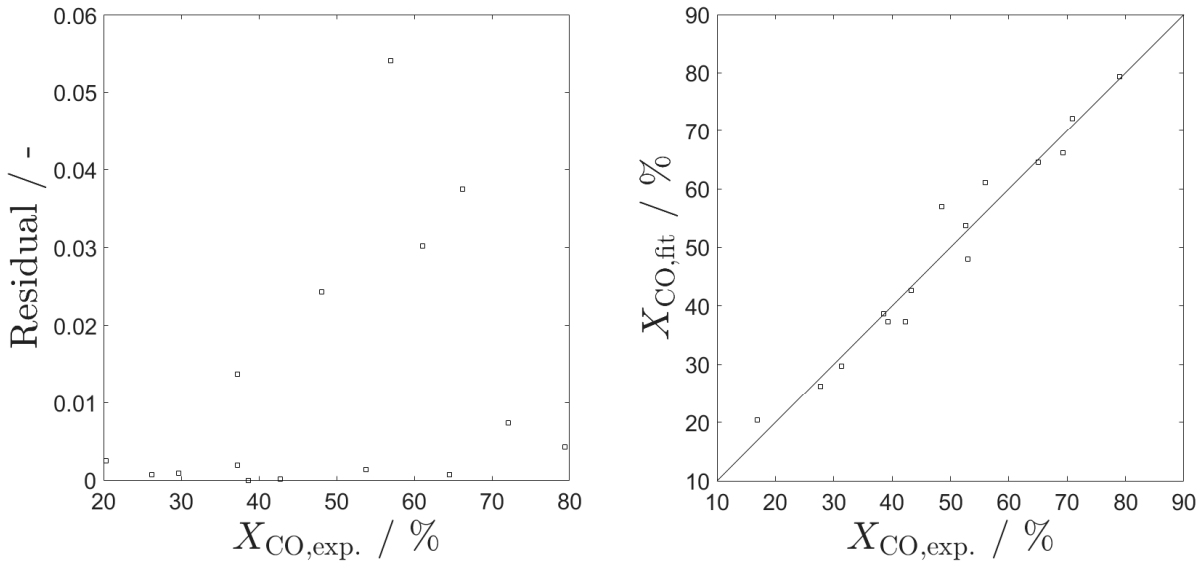

Figure S4: Quality of the fit. Left: Residuals over fitted parameter. Right: Parity plot of experimental and fitted value.

Comparison with Literature

The space time yield can be calculated from gas flow and CO conversion based on equations Eq. 1 and 2. Assumptions Eqs. 3-8 are derived from an ideal Anderson-Schulz-Flory (ASF) product distribution for a chain growth probability of α = 0.85. The values of α and S_{C5+} obtained in experiments confirm these assumptions.

$$STY_{\mathrm{calc}} = X_{\mathrm{CO}} \cdot SV_{\mathrm{mod}} \cdot \rho_{\mathrm{cat}} \cdot y_{\mathrm{CO,in}} \cdot S_{\mathrm{C5+}} \cdot M_{\mathrm{C5+}} \cdot \frac{1}{n_{\mathrm{C5+}} \cdot V_{\mathrm{N}}} \qquad \text{Eq. 1}$$

$$STY_{\mathrm{calc}}/\mathrm{kg_{C5+}\ m_{rct}^{-3}\ h^{-1}} = X_{\mathrm{CO}}/\% \cdot SV_{\mathrm{mod}}/\mathrm{L_N\ g_{cat}^{-1}\ h^{-1}} \cdot 1.226 \qquad \text{Eq. 2}$$

$$\text{With: } \rho_{\mathrm{cat}} = 750\,\frac{\mathrm{kg_{cat}}}{\mathrm{m_{rct}^3}};\ y_{\mathrm{CO,in}} = 0.323;\ S_{\mathrm{C5+}} \approx 0.8; \qquad \text{Eqs. 3-8}$$

$$M_{\mathrm{C5+}} = 151\,\frac{\mathrm{g_{C5+}}}{\mathrm{mol}};\ n_{\mathrm{C5+}} = 10.65;\ V_{\mathrm{N}} = 22.41\,\frac{\mathrm{L_N}}{\mathrm{mol}}$$

The calculated space time yield is depicted in the area generated by modified space velocity and the CO conversion in Figure S5. The STY increases to the top right of the corner. The CO conversion that can be achieved at a certain SV_{mod} and T depends on the catalyst. The activity of the catalysts used are in increasing order: work of Almeida et al. [7], this work, work oy Myrstad et al. [8].

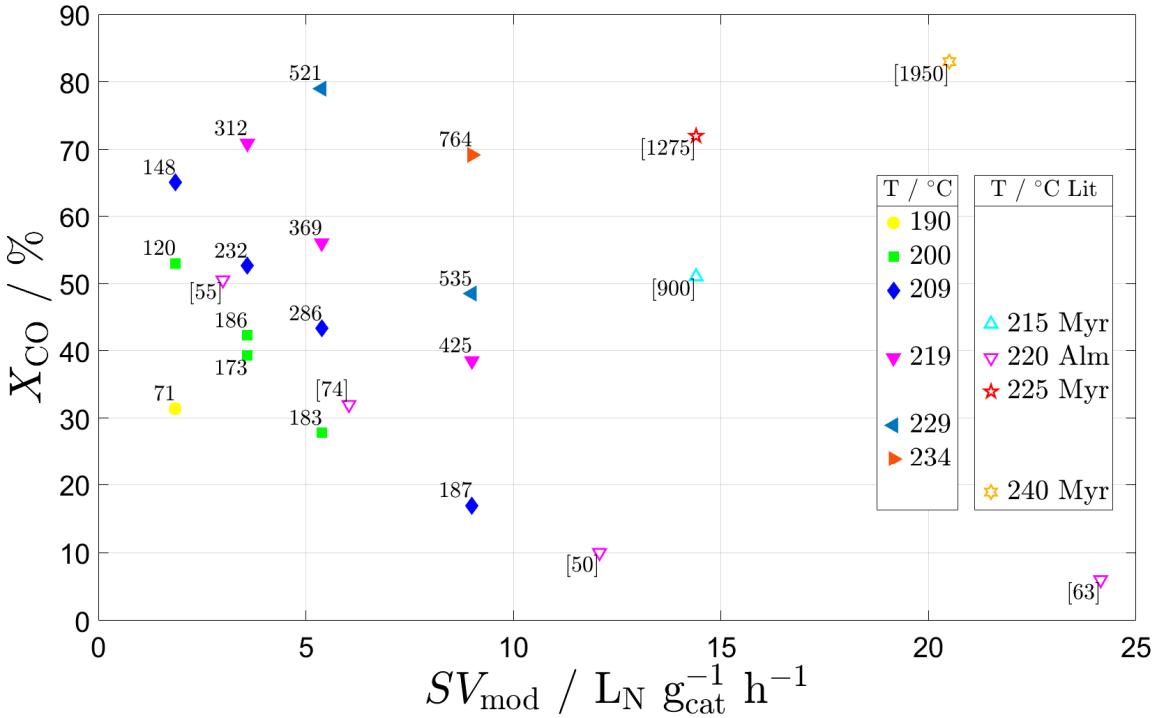

Figure S5: Experimental CO conversion in the plane generated by modified space velocity and temperature with *STY* in kg_{C5+} m_{rct}^{-3} h^{-1} next to the respective data point. Literature values from Almeida et al. and Myrstad et al. [7,8].

In the following Table S3 we make estimations on a scaled-up AM reactor and compare it to industrial FTS reactors. For theses reactors we found data on the productivity per reactor mass *MP* in barrel per day (bpd).

Table S3: Reactor in this work.

Calculation	Comment/Source
P = 3.4 g_{C5+} h^{-1}	
m_{cat} = 3.4 g_{cat}	
STY_{mod} = 1 g_{C5+} g_{cat}^{-1} h^{-1}	With ρ_{cat} = 0.75 g cm^{-3}
STY = 0.75 g_{C5+} cm_{cat}^{-3} h^{-1}	Assuming infinitely extended planar slits, a repetition unit is made up of a reaction slit containing 10 % internal structures, two walls and a cooling slit containing 10 % internal structures. All slits are 1 mm deep and wall thickness is 1 mm. Hence, approx. 2.2 cm^3 metal per cm^3 catalyst are needed. With ρ_{metal} = 8 g cm^{-3} approx. 17.6 g metal per cm^3 catalyst are needed.
MP = 0.0426 g_{C5+} g_{metal}^{-1} h^{-1} = 42.6 kg_{C5+} t^{-1} h^{-1}	
1 bl = 159 L	With ρ = 0.8 kg m^{-3}
1 bl = 127.2 kg	With 24 h d^{-1}
1 bpd (bl per day) = 5.3 kg h^{-1}	
MP = 8.038 bpd t^{-1}	

Table S4: Shell Pearl GTL.

Calculation	Comment/Source
140,000 bpd	[9]
$m_{reactor}$ = 1200 t (24 in total)	[10]
MP = 5833 bpd per reactor = 4.861 bpd t^{-1}	

Table S5: Sasol Oryx GTL.

Calculation	Comment/Source
33,000 bpd	[11]
$m_{reactor}$ = 2000 t (2 in total)	[12]
MP = 16500 bpd per reactor = 8.25 bpd t^{-1}	

A scaled-up version of the AM reactor can produce as much FTS product as an industrial-scale reactor with the equal reactor mass. Compact reactors that are manufactured via complex multi-step manufacturing routes, e.g. diffusion bonding, are researched since ca. 20 years. They are reported to have productivities per reactor mass of *MP* = 13 and 16.5 bpd t^{-1} [13].

Scale-Up

An eight-fold scale-up of the reactor is shown in Figure S6. It would be possible to install about m_{cat} = 30 g.

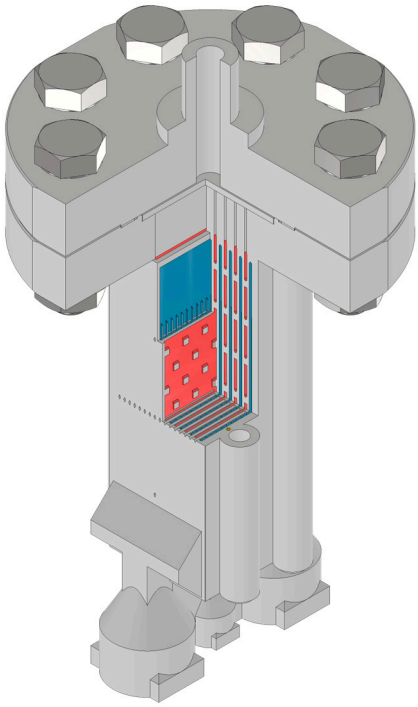

Figure S6: Computer-aided design image of reactor concept for m_{cat} = 30 g.

Evaluation of heat and mass transfer

We evaluated the following criteria to decide whether heat and mass transfer were limiting the chemical reaction. The axial dispersion of mass is insignificant as long as Eq. 9 is fulfilled [14]. The left-hand side equals 380.

$$\frac{l_{\mathrm{cat}}}{d_{\mathrm{p}}} > \frac{8}{Bo_{\mathrm{i}}} \cdot n_{\mathrm{i}} \cdot \ln\left(\frac{1}{1-X_{\mathrm{i}}}\right) \quad \text{Eq. 9}$$

$$\frac{1}{Bo_{\mathrm{i}}} = \frac{\varepsilon_{\mathrm{bed}} \cdot D_{\mathrm{i,m}}}{\tau_{\mathrm{bed}} \cdot d_{\mathrm{p}} \cdot u_0} + 0.5$$

$$\mathrm{i} = \mathrm{H_2}, \mathrm{CO}$$

The internal mass transfer limitation is insignificant if Eq. 10 is fulfilled [15]. Ψ_{WP} is called Weisz-Prater criterion.

$$\Psi_{\mathrm{WP}} = \frac{\left(\frac{d_{\mathrm{p}}}{6}\right)^2 \cdot \frac{n_{\mathrm{i}}+1}{2} \cdot r_{\mathrm{i}}^{\mathrm{V}}}{(1-\varepsilon_{\mathrm{bed}}) \cdot D_{\mathrm{i,eff}} \cdot c_{\mathrm{i,g}}} < 0.15 \quad \text{Eq. 10}$$

$$\mathrm{i} = \mathrm{H_2}, \mathrm{CO}$$

External mass transfer limitation is insignificant as long as Eq. 11 is fulfilled [15].

$$\frac{d_{\mathrm{p}}^2 \cdot r_{\mathrm{i}}^{\mathrm{V}}}{12 \cdot (1-\varepsilon_{\mathrm{bed}}) \cdot D_{\mathrm{i,m}} \cdot c_{\mathrm{i,g}}} < 1 \quad \text{Eq. 11}$$

$$\mathrm{i} = \mathrm{H_2}, \mathrm{CO}$$

The internal heat transfer limitation is insignificant if Eq. 12 is fulfilled [16].

$$\frac{-\Delta H_{\mathrm{R}} \cdot \left(\frac{d_{\mathrm{p}}}{2}\right)^2 \cdot r_{\mathrm{CO}}^{\mathrm{V}}}{(1-\varepsilon_{\mathrm{bed}}) \cdot \lambda_{\mathrm{bed}} \cdot T_{\mathrm{s}}} \cdot \frac{E_A}{\tilde{R} \cdot T_{\mathrm{s}}} < 1 \quad \text{Eq. 12}$$

External heat transfer limitation is insignificant as long as Eq. 13 is fulfilled [16].

$$\frac{-\Delta H_{\mathrm{R}} \cdot \frac{d_{\mathrm{p}}}{2} \cdot r_{\mathrm{CO}}^{\mathrm{V}}}{(1-\varepsilon_{\mathrm{bed}}) \cdot \alpha_{\mathrm{gas}} \cdot T_{\mathrm{s}}} \cdot \frac{E_A}{\tilde{R} \cdot T_{\mathrm{s}}} < 0.05 \quad \text{Eq. 13}$$

Additional values were calculated according to eqs.

$$c_{\mathrm{i}} = \frac{y_{\mathrm{i}} \cdot p}{\tilde{R} \cdot T} \quad \text{Eq. 14}$$

$$\dot{N}_{\mathrm{total}} = \frac{F_{\mathrm{total}}}{V_{\mathrm{N}}} \quad \text{Eq. 15}$$

$$\dot{N}_{\mathrm{CO,conv}} = \dot{N}_{\mathrm{total}} \cdot y_{\mathrm{CO,in}} \cdot X_{\mathrm{CO}} \quad \text{Eq. 16}$$

$$r_{\mathrm{CO}}^{\mathrm{V}} = \frac{\dot{N}_{\mathrm{CO,conv}}}{V_{\mathrm{cat}}};\ r_{\mathrm{H2}}^{\mathrm{V}} = 2 \cdot r_{\mathrm{CO}}^{\mathrm{V}} \quad \text{Eq. 17}$$

$$F_{\mathrm{total}}^{\mathrm{actual}} = F_{\mathrm{total}} \cdot \frac{p_{\mathrm{N}}}{p} \cdot \frac{T}{T_{\mathrm{N}}} \quad \text{Eq. 18}$$

$$u_0 = \frac{F_{\mathrm{total}}^{\mathrm{actual}}}{A_{\mathrm{cross}}} \quad \text{Eq. 19}$$

Table S6: Additional parameters required for criteria calculation.

Parameter	Symbol	Value	Source
Bed length	l_{cat}	0.055 m	
Bed porosity	$\varepsilon_{\mathrm{bed}}$	0.5	
Mixture diffusivity	$D_{\mathrm{H2,m}}$	$6.86 \cdot 10^{-5}$ m² s^{-1}	
Mixture diffusivity	$D_{\mathrm{CO,m}}$	$6.05 \cdot 10^{-5}$ m² s^{-1}	
Bed tortuosity	τ_{bed}	2	
Particle diameter	d_{p}	0.00015 m	
Reaction order	n_{H2}	0.5	
Reaction order	n_{CO}	1	
Effective pore diffusivity	$D_{\mathrm{H2,eff}}, D_{\mathrm{CO,eff}}$	$5 \cdot 10^{-9}$ m² s^{-1}	
Reaction enthalpy	ΔH_{R}	-160000 J mol$_{\mathrm{CO}}^{-1}$	
Bed thermal conductivity	λ_{bed}	1 W m^{-1} K^{-1}	
Activation energy	E_A	100 J mol$_{\mathrm{CO}}^{-1}$	
Inlet molar fraction	y_{H2}	0.646	
Inlet molar fraction	y_{CO}	0.323	
Bed-gas heat transfer coefficient	α_{gas}	5267 W m^{-2} K^{-1}	With λ_{gas} = 0.16 W m^{-1} K^{-1} and Nu_{min} = 5
Molar volume	V_{N}	22.41 L$_{\mathrm{N}}$ mol^{-1}	
Cross-sectional area	A_{cross}	80 mm²	

Table S7: Results of criteria indicate, there is no limitation by heat and mass transfer.

N.	T / °C	SV_{mod} / L_N g_{cat}^{-1} h^{-1}	F_{total} / L_N h^{-1}	X_{CO} / %	X_{H2} / %	c_{H2} / mol m^{-3}	c_{CO} / mol m^{-3}	r_{H2}^V / mol m^{-3} s^{-1}	r_{CO}^V / mol m^{-3} s^{-1}	u_0 / mm s^{-1}	Eq. 9 H2	Eq. 9 CO	Eq. 10 H2	Eq. 10 CO	Eq. 11 H2	Eq. 11 CO	Eq. 12	Eq. 13
1	200	3.59	12.0	39.3	36.7	329	164	8.57	4.28	3.60	59	114	0.00	0.01	1.43E-06	1.62E-06	4.14E-04	1.05E-03
2	209	3.59	12.0	52.6	51.5	322	161	11.45	5.73	3.67	92	167	0.01	0.01	1.94E-06	2.20E-06	5.34E-04	1.35E-03
3	219	3.59	12.0	70.9	72.4	316	158	15.46	7.73	3.75	160	271	0.01	0.01	2.68E-06	3.03E-06	6.91E-04	1.75E-03
4	219	5.38	17.9	56.0	55.8	316	158	18.30	9.15	5.61	68	121	0.01	0.01	3.17E-06	3.59E-06	8.18E-04	2.07E-03
5	229	5.38	17.9	79.0	80.6	310	155	25.80	12.90	5.73	134	226	0.02	0.02	4.56E-06	5.17E-06	1.11E-03	2.81E-03
6	209	5.38	17.9	43.3	41.2	322	161	14.15	7.08	5.50	45	86	0.01	0.01	2.40E-06	2.72E-06	6.59E-04	1.67E-03
7	200	5.38	17.9	27.8	26.5	329	164	9.07	4.54	5.40	27	50	0.01	0.01	1.51E-06	1.71E-06	4.39E-04	1.11E-03
8	209	1.85	6.2	65.1	67.7	322	161	7.31	3.66	1.89	276	453[1]	0.00	0.01	1.24E-06	1.41E-06	3.41E-04	8.62E-04
9	200	1.85	6.2	53.0	53.5	329	164	5.96	2.98	1.86	190	331	0.00	0.00	9.91E-07	1.12E-06	2.88E-04	7.30E-04
10	190	1.85	6.2	31.4	31.2	336	168	3.52	1.76	1.82	95	169	0.00	0.00	5.74E-07	6.51E-07	1.78E-04	4.50E-04
11	209	9.00	30.0	16.9	16.6	322	161	9.23	4.62	9.20	9	17	0.01	0.01	1.57E-06	1.78E-06	4.30E-04	1.09E-03
12	229	9.00	30.0	48.5	50.5	310	155	26.51	13.25	9.58	35	59	0.02	0.02	4.68E-06	5.31E-06	1.14E-03	2.88E-03
13	219	9.00	30.0	38.5	38.4	316	158	21.03	10.52	9.39	25	44	0.01	0.02	3.64E-06	4.13E-06	9.41E-04	2.38E-03
14	234	9.00	30.0	69.2	71.0	307	153	37.82	18.91	9.68	61	103	0.02	0.03	6.75E-06	7.65E-06	1.59E-03	4.03E-03
1R	200	3.59	12.0	42.3	41.2	329	164	9.22	4.61	3.60	68	125	0.01	0.01	1.53E-06	1.74E-06	4.46E-04	1.13E-03

[1] Only incident, where criterion is not fulfilled.

References

1. *DIN EN ISO 4022:2018-12*; Durchlässige Sintermetallwerkstoffe: Bestimmung der Flüssigkeitsdurchlässigkeit. Beuth Verlag GmbH: Berlin, Germany, 2018. Available online: https://www.nautos.de/OJG/search (accessed on 20.08.2023).
2. Kirsch, H. Dezentrale Synthese Strombasierter Flüssiger Kraftstoffe über die Fischer-Tropsch Route. Doctoral Dissertation, Karlsruher Institut für Technologie: Karlsruhe, Germany, 2020. https://doi.org/10.5445/IR/1000129949
3. Flory, P.J. Molecular Size Distribution in Linear Condensation Polymers. *J. Am. Chem. Soc.* **1936**, 58, 1877–1885. https://doi.org/10.1021/ja01301a016
4. Kaiser, R. E. *Gas-Chromatographie*. 2. Aufl. Bd. 22. B I Hochschultaschenbücher. Mannheim: Bibliogr. Inst, 1973. ISBN: 3-411-00022-8.
5. Brübach, L.T. Katalytische Hydrierende Spaltung von Fischer-Tropsch Produkten im Technikumsmaßstab. Master's Thesis, Karlsruher Institut für Technologie, Karlsruhe, Germany, 2018.
6. Pabst, K.; González, M.I.; Kraushaar-Czarnetzki, B.; Schaub, G. Combination of Fischer–Tropsch Synthesis and Hydroprocessing in a Single-Stage Reactor. Part I. Mathematical Modeling of the Reaction Kinetics. *Ind. Eng. Chem. Res.* **2013**, *52*, 8978–8987. https://doi.org/10.1021/ie303047a
7. Almeida, L.C.; Echave, F.J.; Sanz, O.; Centeno, M.A.; Arzamendi, G.; Gandía, L.M.; Sousa-Aguiar, E.F.; Odriozola, J.A.; Montes, M. Fischer–Tropsch synthesis in microchannels. *Chem. Eng. J.* **2011**, *167*, 536–544. https://doi.org/10.1016/j.cej.2010.09.091.
8. Myrstad, R.; Eri, S.; Pfeifer, P.; Rytter, E.; Holmen, A. Fischer–Tropsch synthesis in a microstructured reactor. *Catal. Today* **2009**, *147*, S301–S304. https://doi.org/10.1016/j.cattod.2009.07.011.
9. Shell. Pearl GTL Overview. Available online: https://www.shell.com/about-us/major-projects/pearl-gtl/pearl-gtl-an-overview.html (accessed on 3 July 2023).
10. MAN Energy Solutions. Shell Pearl GTL—Gas-to-liquid reactor in Qatar for Shell. Available online: https://www.man-es.com/process-industry/products/chemical-reactors/water--air--oil-operated-reactors (accessed on 3 July 2023).
11. Hydrocarbons Technology. Oryx. Available online: https://www.hydrocarbons-technology.com/projects/oryx/ (accessed on 3 July 2023).
12. Technip. Oryx GTL, 2011. Available online: https://docplayer.net/45263490-Our-projects-oryx-gtl.html (accessed on 25 August 2023).
13. Selinsek, M. Compact Fischer-Tropsch Synthesis in Gas-to-Liquid Applications. In Proceedings of the 2nd Thematic Workshop, Prague and Litvinov, Czech Republic, 23–24 May 2019. Available online: https://www.comsynproject.eu/publications/ (accessed 20 August 2023).
14. Berger, R. EUROKIN Spreadsheet on Requirements for Measurement of Intrinsic Kinetics in the Gas-Solid Fixed-Bed Reactor, 2010. Available online: https://eurokin.org/wp-content/uploads/downloads/2019/08/EUROKIN_fixed-bed_html_guide.pdf (accessed on 15 September 2023).
15. Jess, A.; Wasserscheid, P. *Chemical Technology*: *An Integral Textbook;* Wiley-VCH: Weinheim, Germany, 2013; ISBN 978-3-527-30446-2.
16. Pfeifer, P. Application of catalysts to metal microreactor systems. In *Chemical Kinetics*; Patel, V., Ed.; InTech Europe: Rijeka, Croatia, 2012; pp 325–345, ISBN 978-953-51-0132-1.

Nomenclature

Latin symbols

A	Area (mm)
F	Volumetric flow rate (L_N h^{-1})
$\widetilde{M}$	Molar mass (kg mol^{-1})
MP	Productivity per reactor mass (bpd t^{-1})
m	Mass (kg)
$\dot{N}$	Molar flow (mol s^{-1})
n_C	Number of carbon atoms (-)
P	Productivity of C5+ (kg s^{-1}; g h^{-1})
p	Pressure (bar)
S	Selectivity (mol/mol)
STY	Space time yield (kg m^{-3} h^{-1})
SV	Space velocity at normal conditions (L_N m^{-3} h^{-1})
T	Temperature (°C; K)
TOS	Time on stream (h)
V	Volume (mm^3)

t	Thickness, dimension (mm)
X	Conversion (-)
y	Molar fraction (mol/mol)
Greek symbols	
α	Chain growth probability (-)
Δ	Difference (div.)
ε	Porosity (-)
Ψ	Permeability coefficients (m^{-1}; m^{-2})
ω	Weight fraction (kg/kg)
Subscript	
cat	Catalyst
I	Inertia permeability coefficient
mod	Modified, in this work: related to catalyst mass
N	Normal conditions (p = 1.01325 bara, T = 273.15 K)
p	Particle, pin
V	Permeability coefficient of flow